



Molecular Crystals and Liquid Crystals Science and Technology. Section A. Molecular Crystals and Liquid Crystals

Publication details, including instructions for authors and
subscription information:

<http://www.tandfonline.com/loi/gmcl19>

Static and Dynamic Characteristics of Field Induced Antiferroelectric- Ferroelectric Phase Transition

Hiroshi Moritake^a, Keizo Nakayama^{a,b}, Masanori Ozaki^a & Katsumi
Yoshino^a

^a Department of Electronic Engineering, Faculty of Engineering,
Osaka University 2-1 Yamada-Oka, Suita, Osaka, 565, JAPAN

^b Nara National College of Technology, 22 Yatacho, Yamatokoriyama,
Nara, 639-11, JAPAN

Version of record first published: 23 Sep 2006.

To cite this article: Hiroshi Moritake, Keizo Nakayama, Masanori Ozaki & Katsumi Yoshino (1995):
Static and Dynamic Characteristics of Field Induced Antiferroelectric-Ferroelectric Phase Transition,
Molecular Crystals and Liquid Crystals Science and Technology. Section A. Molecular Crystals and
Liquid Crystals, 263:1, 13-26

To link to this article: <http://dx.doi.org/10.1080/10587259508033566>

PLEASE SCROLL DOWN FOR ARTICLE

Full terms and conditions of use: <http://www.tandfonline.com/page/terms-and-conditions>

This article may be used for research, teaching, and private study purposes. Any
substantial or systematic reproduction, redistribution, reselling, loan, sub-licensing,
systematic supply, or distribution in any form to anyone is expressly forbidden.

The publisher does not give any warranty express or implied or make any representation
that the contents will be complete or accurate or up to date. The accuracy of any
instructions, formulae, and drug doses should be independently verified with primary
sources. The publisher shall not be liable for any loss, actions, claims, proceedings,
demand, or costs or damages whatsoever or howsoever caused arising directly or
indirectly in connection with or arising out of the use of this material.

STATIC AND DYNAMIC CHARACTERISTICS OF FIELD INDUCED ANTIFERROELECTRIC-FERROELECTRIC PHASE TRANSITION

HIROSHI MORITAKE, KEIZO NAKAYAMA*, MASANORI OZAKI
and KATSUMI YOSHINO

Department of Electronic Engineering, Faculty of Engineering, Osaka University
2-1 Yamada-Oka, Suita, Osaka 565, JAPAN

ABSTRACT The light scattering measurement and the polarized microscopic observation of field induced phase transition between antiferroelectric (AF) and ferroelectric (F) phases have been performed in a uniformly aligned cell. The light scattering is confirmed to be diffraction by the periodical change in refractive index in the stripe domains of AF and F phases. In $F \rightarrow AF$ phase transition, the nucleation of AF domain occurs at interfaces between liquid crystal and spacer edges and AF domain grows away from spacers. On the other hand, in $AF \rightarrow F$ phase transition, discrete F domains homogeneously appear and grow throughout the cell. The rotation of smectic layer is also observed under the application of an asymmetric voltage. This rotation is originated from the asymmetry of the polarity reversal of the applied voltage.

INTRODUCTION

Since the discovery of antiferroelectricity in 4-(1-methylheptyloxycarbonyl) phenyl 4'-octyloxybiphenyl-4-carboxylate (MHPOBC),¹ antiferroelectric liquid crystal (AFLC) has attracted considerable attention from both fundamental and practical points of view. From fundamental point of view, tristable switching, dielectric properties, existence of some subphases and so on have been reported.²⁻⁶ On the other hand, from practical point of view, some applications such as display have been proposed.^{7,8} In these

*Permanent address: Nara National College of Technology,
22 Yatacho, Yamatokoriyama, Nara 639-11, JAPAN

applications, the field induced phase transition between antiferroelectric (AF) and ferroelectric (F) phases has been utilized as the origin of the switching. In this paper, we report the characteristics of field induced phase transition between AF and F phases by means of light scattering measurement and polarized microscopic observation using stroboscopic technique. In addition, anomalous smectic layer rotation by applying an asymmetric voltage in the AF phase is also reported.

EXPERIMENTAL

AFLC material used in this study was 4-(1,1,1-trifluoromethyl-heptyloxycarbonyl) phenyl 4'-octyloxybiphenyl-4-carboxylate (TFMHPOBC) which indicates following phase sequence: Iso. - SmA - SmC_A*.⁹ The sample was sandwiched between two In-Sn oxide (ITO) coated conducting glass plates whose surfaces were not treated with any surfactant such as polymers, which was fixed by polyethyleneterephthalate (PET) sheets as spacers. Monodomain and multidomain cells of homogeneous alignment were used in this study. The unidirectionally aligned monodomain was obtained by gradually growing the smectic domain from the edge of a spacer with the assistance of thermal gradient.¹⁰ In this type cell, PET sheets as spacers were set in keeping the distance of 0.1-1 mm on ITO electrodes and electric field was applied in whole area of the sample.

For the measurement of light scattering, a He-Ne laser (632.8 nm) was used as a light source and no polarizers were used. The transmitted light intensity through the cell was monitored with a photodiode. For the observation of azimuthal angle dependence of scattered light intensity, a screen was set instead of the photodiode. The applied voltage was modulated by a function generator (HP, 3314A or YOKOGAWA, AG-1200) and amplified by a power amplifier (NF, 4010). The switching process of the field induced phase transition was observed under the polarized microscope adopting the stroboscopic technique. The direction of the molecular alignment and its quality were measured by the polarized microscopic observation.

RESULTS AND DISCUSSION

Light Scattering at Field Induced Phase Transition

The transmission light through the cell was scattered at the field induced phase transition.¹¹ The response waveforms of the transmission light intensity to applied voltage of the triangular wave at various frequencies were measured. Figure 1 shows three typical response waveforms of transmitted light intensity. Figure 1 shows these response waveforms. At low frequency, two dips of the transmission intensity were observed as shown in Figure 1(a). One appeared at negative voltage and the other appeared at positive voltage, which correspond to the threshold voltages of $F(-) \rightarrow AF$ and $AF \rightarrow F(+)$ phase transitions, respectively ($F(-)$ means the ferroelectric state realized by the application of negative voltage). As frequency increased, a new sharp dip of transmission intensity appeared at around zero voltage in addition to two dips as shown in Figure 1(b). This additional sharp dip is due to the transient scattering which is caused by direct transition between two ferroelectric uniform states.¹¹ That is, $F(-) \rightarrow AF$ phase

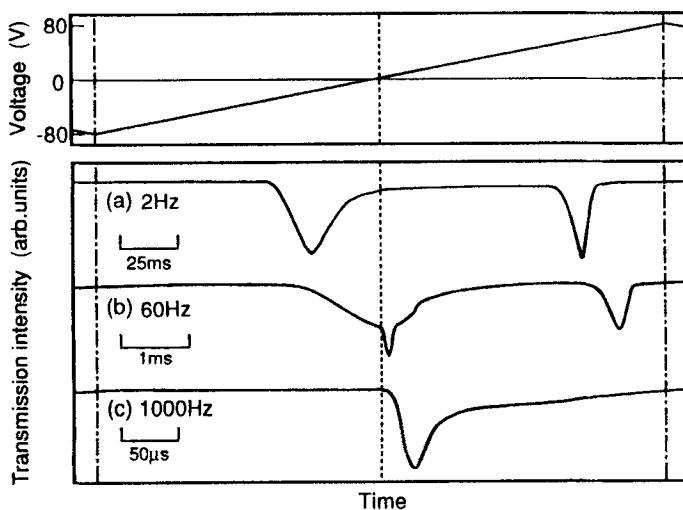


Figure 1 Typical waveforms of the transmission light intensity to applied voltage of triangular wave as a function of frequency ((a) 2 Hz, (b) 60 Hz and (c) 1000 Hz) in the SmC_A^* phase at 5° C below the $SmA - SmC_A^*$ transition temperature.

transition occurs just before crossing 0 V and the voltage crosses zero before F(-)→AF transition completely finishes. In other words, the voltage crosses zero in the middle of F(-)→AF transition. As the result, when the polarity reverses, residual F(-) state turns into F(+) state. Finally, since the AF state must be established at low voltage, F(+) state turns into AF state.

As frequency increased further, only one dip in transmission intensity was observed as shown in Figure 1(c). This dip originates in the direct transition between two F uniform states because the rate of voltage change was too rapid and the AF phase did not appear.

The light scattering due to the field induced phase transition between the AF and F phases is attributed to the periodical change in the refractive index in the stripe domains of the F and AF phases along the smectic layer.⁴ Therefore, the transmitted light should be scattered along the layer normal direction by this field induced phase transition. When a unidirectionally aligned cell is used in this measurement, the azimuthal angle dependence of the scattered light should be observed. Figure 2 shows scattering image and polarizing microphotograph at the field induced AF→F(+) phase transition. The transmitted light indicates the azimuthal angle dependence and is scattered perpendicular to the layer. This agrees with the light scattering due to the periodical change in the refractive index in the stripe domains. The scattered light perpendicular to the layer has

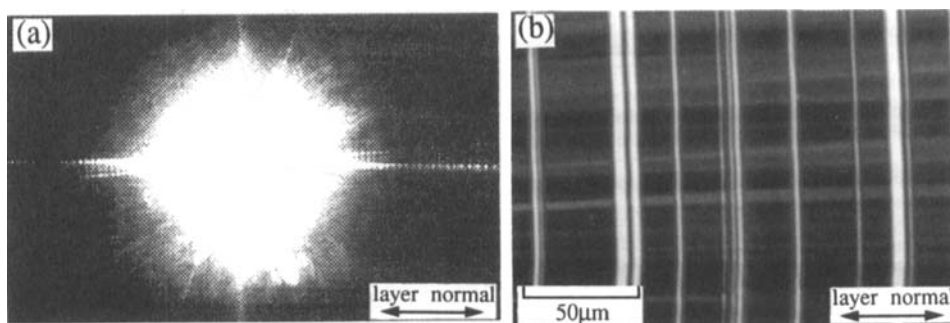


Figure 2(a) Transmitted light pattern and (b) polarized microphotograph at field induced AF-F phase transition using the unidirectionally aligned cell. See Color Plate I.

the periodical change in brightness. This periodical change of brightness in the profile of scattered light suggests that the transmitted light is diffracted by the periodical change in refractive index in the stripe domains of AF and F phases. To compute the period of the AF and F regions, Fourier transform of the profile of transmitted light in the direction perpendicular to the layer was carried out. The result is shown in Figure 3. From this figure, the period of the AF and F regions was estimated to be about 30 μm . It has been confirmed that the light scattering at the field induced phase transition between AF and F phases is due to the periodical change in the refractive index in the stripe domain.

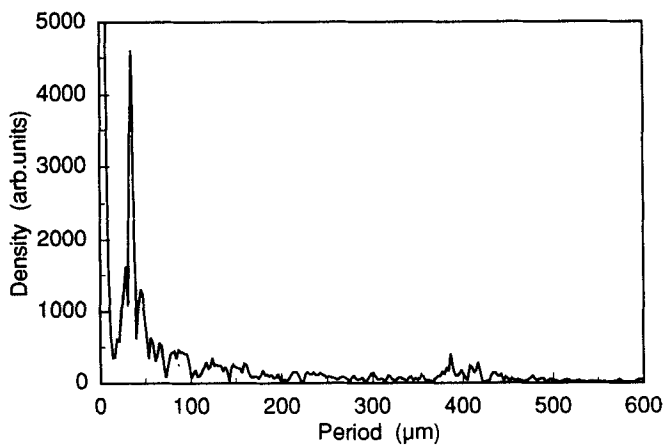


Figure 3 Fourier transform of the profile of transmitted light in the direction perpendicular to the layer.

Characteristic of Field Induced Phase Transition

To investigate the characteristics of field induced phase transition to various applied voltage waveforms, the stroboscopic observation of uniformly aligned cell at the field induced phase transition with the polarized microscope was carried out. Figure 4 shows a series of microphotographs at several voltages under applying triangular voltage at the frequency of 5 Hz. As shown in Figures 4(a) and 4(b), the F \rightarrow AF phase transition was accompanied with the nucleation of the AF domains at interfaces between liquid crystal and spacer edges, that is, the AF domains grew away from spacers. The clear domain

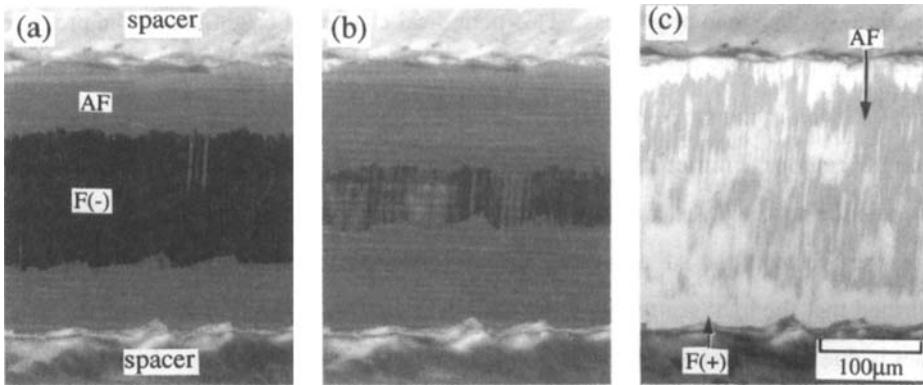


Figure 4 Polarized microphotographs at $F(-) \rightarrow AF$ transition ((a) -9 V and (b) -2 V) and $AF \rightarrow F(+)$ transition ((c) 41 V) to applied voltage of triangular wave in frequency of 5 Hz. See Color Plate II.

walls parallel to spacers moved toward the center of sample cell.

On the other hand, in the $AF \rightarrow F$ phase transition, besides the growth of F domain from spacer edges, discrete F domains homogeneously appeared and grew throughout the cell, as shown in Figure 4(c). The distinct domain wall parallel to spacers was not observed.

As frequency of triangular voltage waveform increases, the $F(-) \rightarrow AF$ phase transition occurs at low negative voltage. When the voltage crosses zero before this transition completely finishes, the residual $F(-)$ state turns to the $F(+)$ state as mentioned above. A series of microphotographs at various voltages under applying the triangular waveform at the frequency of 20 Hz is shown in Figure 5. When the voltage increased and reached the low negative voltage at which the phase transition occurred, the $F(-) \rightarrow AF$ phase transition occurred as the same manner at low frequency before the voltage crossed zero. That is, the $F(-) \rightarrow AF$ transition was accompanied with the nucleation of the AF domains at interfaces between liquid crystal and spacer edges (Figure 5(a)). On the other hand, when voltage crossed zero and the polarity reversed at that instant, the polarization of the residual $F(-)$ state (center of the cell) reversed and $F(-) \rightarrow F(+)$ transition occurred. The $F(-) \rightarrow F(+)$ transition occurred homogeneously throughout

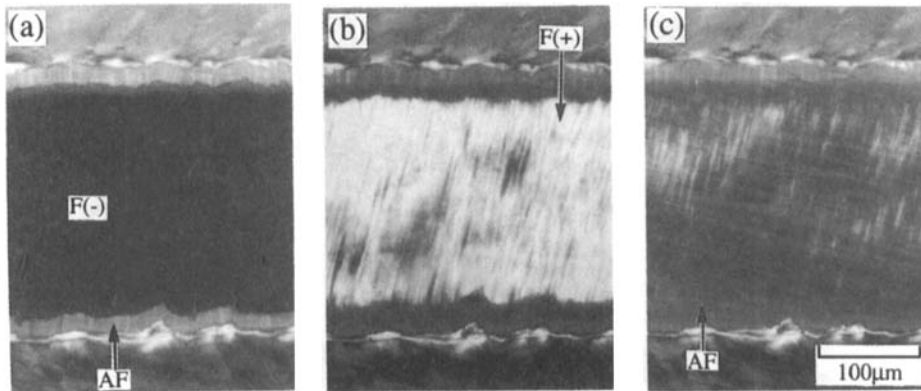


Figure 5 Polarized microphotographs at $F(-) \rightarrow AF$ transition ((a) -6 V, (b) 1 V and (c) 4 V) to applied voltage of triangular wave in frequency of 20 Hz.

See Color Plate III.

residual $F(-)$ state (Figure 5(b)). But the AF state must be established at low voltage so that $F(+)$ state turned into the AF state, as shown in Figure 5(c). As is evident from this microphotograph, the discrete AF domains appeared and grew throughout the center of cell.

If the $F(+)$ state is completely established, the $F(+)$ \rightarrow AF phase transition should occur as the domain walls between $F(+)$ and AF phase move toward the center of sample cell. However, in the $F(+)$ \rightarrow AF phase transition, the discrete AF domains appeared homogeneously. This suggests that $F(+)$ state was not completely established and the nucleation and growth of the AF domain occurs in the center of cell during the direct $F(-) \rightarrow F(+)$ phase transition. The voltage increased further, the AF $\rightarrow F(+)$ phase transition occurred homogeneously through the cell as the same manner at low frequency.

The observation of field induced phase transition using the stepwise voltage pulse was carried. Figure 6 shows a series of microphotographs of $F(-) \rightarrow AF$ transition after changing the voltage stepwise from -60 V to 0 V. As shown in Figure 6(a), the nucleation of the AF domain occurred at interfaces between liquid crystal and spacer edges as the same manner under applying triangular voltage. The AF domain grew along the layer though the clear domain wall parallel to spacer was not observed. In this case, a few discrete AF domains were also observed in the center of cell as shown in Figure

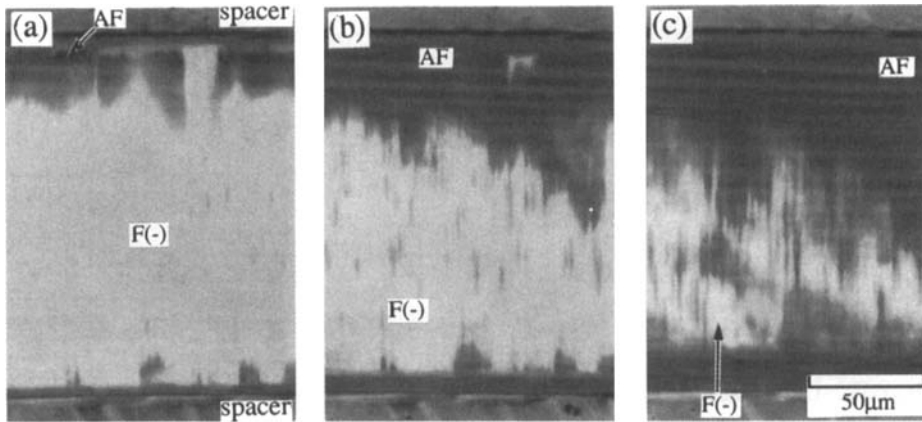


Figure 6 Polarized microphotographs at $F(-) \rightarrow AF$ transition after changing the voltage stepwise from -60 V to 0 V (after (a) $300 \mu s$, (b) $600 \mu s$ and (c) $1200 \mu s$). See Color Plate IV.

6(b).

At the $F \rightarrow AF$ phase transition, most of AF domain grow away from spacers though the $AF \rightarrow F$ phase transition occurs homogeneously. To estimate the growth velocity of AF domain along the layer, the average distance between AF-F domain wall and the spacer was obtained from the microphotographs at $F \rightarrow AF$ transition. Figure 7 shows the ratio of this average distance to the distance between two spacers as a function of time after changing the voltage from -60 V to 0 V (denoted as closed circles) and under applying the triangular voltage (denoted as closed circles). In the case of changing the voltage stepwise to 0 V, the ratio is proportional to time. This suggests that the growth velocity of AF domain is constant under applying the constant voltage. On the other hand, the growth velocity of AF domain under applying the triangular voltage increases as time increases. Under applying the triangular voltage, the applied voltage is not constant and the difference between applied voltage and threshold voltage increases with time. Therefore, the increase of the growth velocity may be due to the increase of differential voltage between applied and threshold voltages.

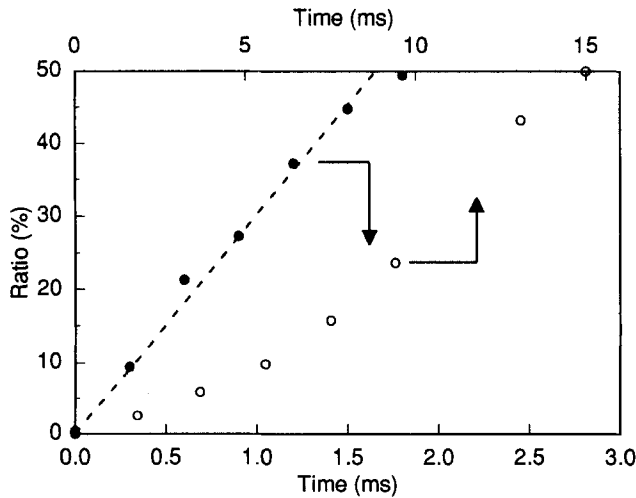


Figure 7 The ratio of the average distance between AF-F domain wall and the spacer to the distance between two spacers as function of time after changing the voltage stepwise from -60 V to 0 V (denoted as closed circles) and under applying the triangular voltage at frequency of 5 Hz (denoted as open circles).

Smectic Layer Rotation

The rotation of the smectic layer is observed under the application of an asymmetric voltage.¹² Figure 8 shows the rotate angle with respect to the initial alignment direction as a function of the number of voltage pulse trains. The waveform of applied voltage pulse used in this measurement is also shown in this figure. This waveform consists of three time segments. Two segments are the constant voltages with negative and positive polarities and are denoted as V_{p-} and V_{p+} , respectively. These two constants voltages are connected with the ramp voltage whose duration is denoted as T_r . The rotate angle ϕ increases with increasing the number of pulse trains N and ϕ is proportion to N below about 25° of ϕ . In this range, the smectic layer rotates homogeneously throughout the sample and the uniformity of the alignment is maintained. However, the sample was divided into several domains over 25° of ϕ .

In this waveform of applied voltage, two asymmetries are included. One is the

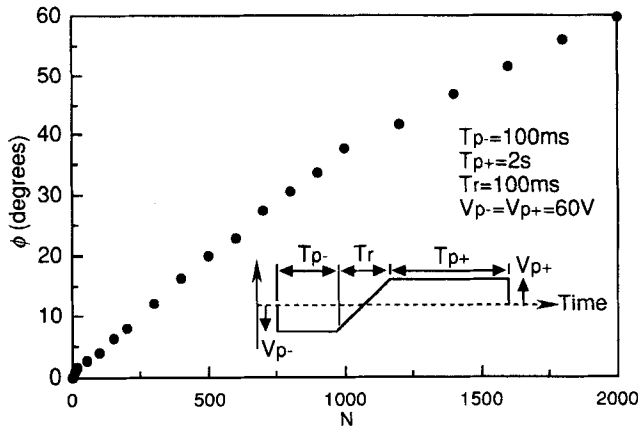


Figure 8 Rotate angle of the smectic layer with respect to the initial alignment direction as a function of the number of voltage pulse trains and the waveform of applied voltage pulse used in this measurement.

existence of the ramp voltage which is introduced only in the segment from T_{p-} to T_{p+} , and the other is difference of durations of constant voltages V_{p-} and V_{p+} . To clarify which asymmetry contributes to the layer rotation, two types of waveforms in which one of two asymmetries is removed from the waveform were applied. When the step-wise voltage pulse was applied (removal to ramp voltage), the layer did not rotate as shown in Figure (denoted as open circles). While, when the voltage pulse whose T_{p-} and T_{p+} are equal is applied (removal of difference between T_{p-} and T_{p+}), the layer rotates as shown

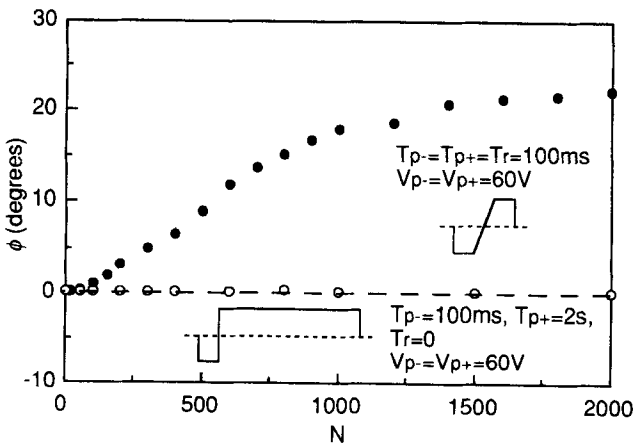


Figure 9 Rotate angle of the smectic layer as a function of the number of voltage pulse trains using the voltage waveforms in which one of two asymmetries is removed.

in Figure 9 (denoted as closed circles). This result suggests that the asymmetry of durations between the negative and positive voltages is not necessary to layer rotation. Therefore, the uniform layer rotation must originate from the asymmetry of the polarity reversal of the applied voltage.

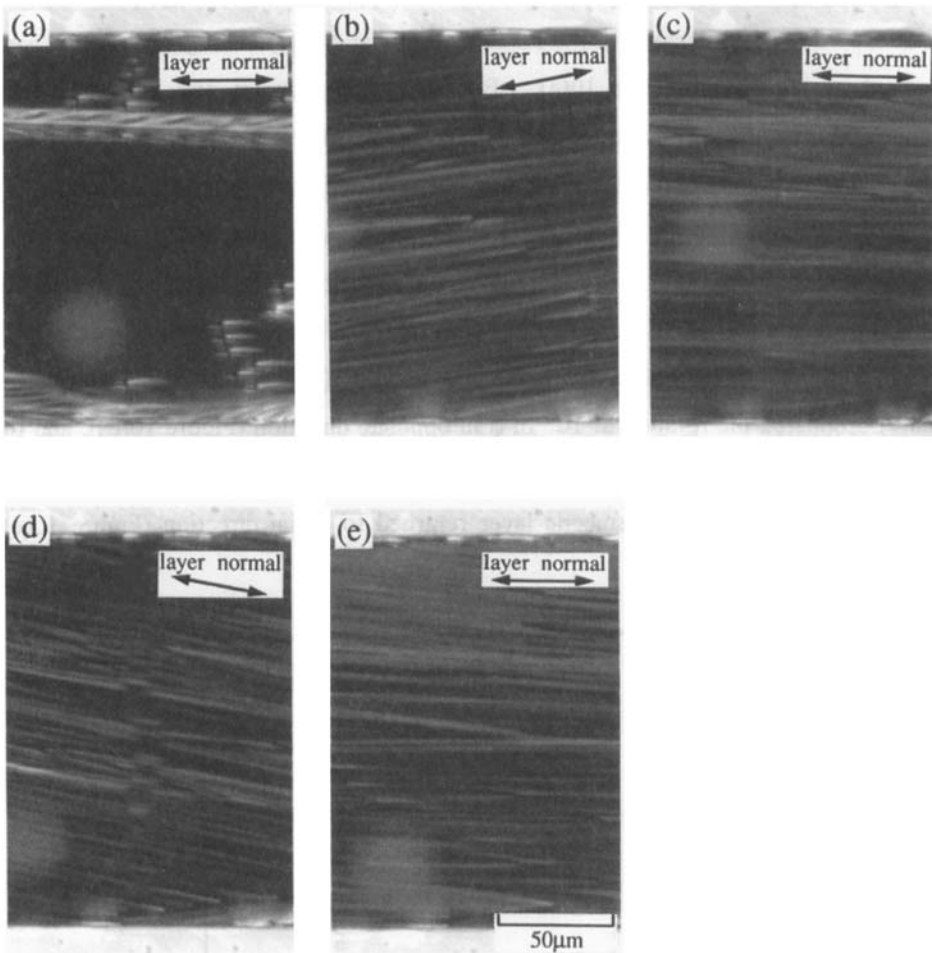


Figure 10 A series of photomicrographs in the measurement of rotate angle ϕ of the smectic layer when the polarity of the waveform ($T_{p-}=T_{p+}=T_r=100\text{ms}$, $V_p=60\text{V}$) was changed at 500 and 1500 cycles. (a) The initial state before the measurement. After the application of voltage pulse of (b) 500 cycles, (c) 1000 cycles, (d) 1500 cycles and (e) 2000 cycles. See Color Plate V.

If the polarity of the waveform of the applied pulse is inverted with respect to 0 V, the smectic layer should rotate to the opposite direction. To confirm that the rotation of the smectic layer is reversible, the measurement of the rotate angle ϕ as a function of N was carried out when the polarity of the waveform of the applied pulse ($T_{p-} = T_r = T_{p+} = 100\text{ms}$) changes at 500 and 1500 cycles. Figure 10 shows a series of microphotographs in the initial state and after the application of voltage pulses of 500, 1000, 1500 and 2000 cycles. In the initial state, focal conics and zig-zag defects were observed as shown in Figure 10(a). But these focal conics and zig-zag defects disappeared after the application of one voltage pulse. After the application of voltage pulse of 500 cycles, the direction of the smectic layer uniformly rotated at about 10° of ϕ as shown in Figure 10(b). While, after applying the voltage pulse 500 cycles in reverse polarity (application of 1000 cycles in totality), the direction of the smectic layer returned to initial direction (0° of ϕ), as shown in Figure 10(c). Furthermore, the application of voltage pulse of more 500 cycles in reverse polarity (application of 1500 cycles in totality) originated the rotation at 10° of ϕ in opposite direction (Figure 10(d)), and the application of voltage pulse of 500 cycles in initial polarity (application of 2000 cycles in totality), the direction of the smectic layer returned to initial direction (Figure 10(e)).

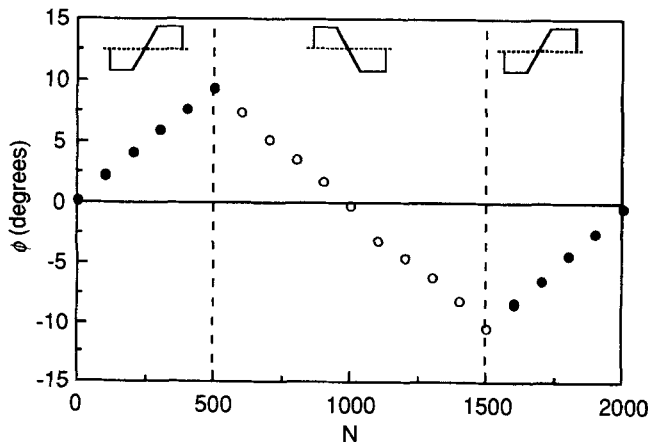


Figure 11 Rotate angle of the smectic layer as a function of the number of voltage pulse trains using the voltage waveform ($T_{p-} = T_{p+} = T_r = 100\text{ms}$, $V_p = 60\text{V}$). The polarity of the waveform is changed at 500 and 1500 cycles.

The uniform rotation of the smectic layer to both directions is confirmed from these figure. Figure 11 shows the rotate angle ϕ as a function of N . As shown in Figure 11, the rotate angle ϕ is linear to N . One pulse of applied voltage rotates the layer by 0.2° for both polarities of applied voltage pulse. It should be noted that the uniformity of the alignment is maintained after the voltage application of 2000 cycles which causes the layer rotation to the total angle of about 40° , as shown in Figure 10(e). It is confirmed that the rotation of smectic layer is reversible and occurs by the exactly same rate to one pulse of applied voltage in both polarities.

SUMMARY

The light scattering which was observed at the field induced phase transition between AF and F phases was confirmed to be diffraction by the periodical change in refractive index in the stripe domains of AF and F phases. The polarized microscopic observation of the field induced phase transition under applying triangular voltage and stepwise voltage was carried out. At $F \rightarrow AF$ phase transition, the nucleation of the AF domain occurred at interfaces between liquid crystal and spacer edges and the AF domain grew away from spacers. In particular, at low frequency of triangular voltage, the clear domain walls parallel to spacer which moved toward the center of sample were observed. The growth velocity of AF domain along the layer was depend on the voltage. On the other hand, in the $AF \rightarrow F$ phase transition, discrete F domains homogeneously appeared and grew throughout the cell. The rotation of smectic layer was observed under the application of an asymmetric waveform of the voltage. This rotation was originated from the asymmetry of the polarity reversal of the applied voltage. The direction of this rotation was decided by the polarity of applied voltage pulse and this rotation was reversible.

REFERENCES

1. A. D. L. Chandani, E. Gorecka, Y. Ouchi, H. Takezoe and A. Fukuda, Jpn. J. Appl. Phys., **28**, L1265 (1989).
2. M. Johno, K. Itoh, J. Lee, Y. Ouchi, H. Takezoe, A. Fukuda and T. Kitazume,

- Jpn. J. Appl. Phys., 29, L107 (1990).
3. E. Gorecka, A. D. L. Chandani, Y. Ouchi, H. Takezoe and A. Fukuda, Jpn. J. Appl. Phys., 29, 131 (1990).
 4. H. Moritake, N. Shigeno, M. Ozaki and K. Yoshino, Jpn. J. Appl. Phys., 31, 3193 (1992).
 4. H. Moritake, N. Shigeno, M. Ozaki and K. Yoshino, Liq. Cryst., 14, 1283 (1993).
 5. K. Hiraoka, Y. Ouchi, H. Takezoe and A. Fukuda, Mol. Cryst. Liq. Cryst., 199, 197 (1991).
 6. H. Moritake, Y. Uchiyama, K. Myojin, M. Ozaki and K. Yoshino, Ferroelectrics, 147, 53 (1993).
 7. Y. Yamada, N. Yamamoto, K. Mori, K. Nakamura, T. Hagiwara, Y. Suzuki, I. Kawamura, H. Orihara and Y. Ishibashi, Jpn. J. Appl. Phys., 29, 1757 (1990).
 8. N. Yamamoto, N. Koshoubu, K. Mori, K. Nakamura, Y. Yamada, Ferroelectrics, 149, 295 (1993).
 9. K. Yoshino, M. Ozaki, H. Taniguchi, N. Yamasaki, K. Satoh, Liq. Cryst., 5, 1203 (1989).
 10. K. Kondo, H. Takezoe, A. Fukuda and K. Kuze, Jpn. J. Appl. Phys., 22, L85 (1993).
 11. H. Moritake, S. Cho, M. Ozaki and K. Yoshino, Jpn. J. Appl. Phys., 32, L1549 (1993).
 12. M. Ozaki, H. Moritake, K. Nakayama and K. Yoshino, submitted to Phys. Rev. Lett..